INFLUENCE OF ALBUMIN ON THE CORROSION BEHAVIOR OF Ti50Zr ALLOY

Radu NARTITA[1], Daniela IONITA[2]

Considering the complex process of corrosion that takes place in biological electrolytic solutions we have investigated the influence of albumin on the corrosion behavior of a titanium-zirconium alloy. The study was performed through electrochemical and spectroscopic analysis. Electrochemical stability was evaluated using potentiodynamic polarization and electrochemical impedance spectroscopy. The adsorption of albumin on the alloy surface was investigated spectrophotometrically and the concentrations of metal ions released in the solution were measured by inductively coupled plasma mass spectrometry. The results obtained indicate that albumin forms a protective layer on the surface, inhibiting the corrosion process.

Keywords: titanium zirconium alloy, albumin, electrochemical stability.

1. Introduction

Alloying Titanium (Ti) with Zirconium (Zr) leads to the formation of biomaterials with enhanced properties compared to the individual metallic constituents [1, 2]. Moreover, due to their nature, different types of nanostructures can be created on TiZr alloys [3]. The nanostructures created increase the surface roughness which can lead to improved osseointegration, better corrosion resistance and better overall biocompatibility [4].

Additionally, avoiding peri-implant infections, that can lead to implant failure, is of utmost importance [5]. Therefore, many techniques were developed in the last years to obtain reduced bacterial adhesion, antibacterial or anti-inflammatory properties and greater corrosion resistance [6–8].

The passive oxide layer formed naturally on some metals or alloys confers improved biocompatibility contributing to better corrosion resistance, but the native film is not very thick. However, it can be improved through various methods [9, 10]. Corrosion of the metallic biomaterials in the biological electrolytic solutions that contain both ions and biomolecules is a very complex process [11]. Albumin is one of the proteins found in high concentration in plasma

[1] PhD student., Dept. of General Chemistry, University POLITEHNICA of Bucharest, Romania, email: nartita.radu@gmail.com [2]

[2] Prof., Dept. of General Chemistry, University POLITEHNICA of Bucharest, Romania, e-mail: md_ionita@yahoo.com

and therefore the effect resulted from the initial interaction is a key factor in determining the performance of the biomaterial [12].

The mechanism of interaction varies depending on several factors, the albumin can either be adsorbed on the metallic surface forming a layer or it can form organometallic bounds with the metallic species presented at the surface. Other possible mechanisms include the reduction of albumin at the surface by redox reaction or formation of organometallic complexes in the solution, that can precipitate on the surface after reaching a critical concentration [13]. Considering these complex mechanisms it is clear that proteins can both promote and inhibit the corrosion of metallic alloys [14, 15].

In the case of titanium alloys, the protein adsorption mechanism can be described as an interaction between the hydroxylated surface and the negatively charged carboxyl groups of the proteins. However, there is not a generally accepted mechanism due to the large number of factors that can lead to a different behavior [16]. The main contributing factors to the opposed behaviors are represented by the bulk composition, and the surface and subsurface structure [17–21].

In the *in vitro* studies conducted, it is shown that albumin can have either a negative or a positive influence on corrosion behavior [15, 22]. It is important to note that short term studies that highlight an improved corrosion resistance could have different results after extended periods [23].

Even if the Ti50Zr alloy is considered a bioinert alloy, small quantities are released in the surrounding tissue and the body. The metal ions released in the corrosion process can pose a threat to human health [24]. Therefore, understanding the complex interactions that take place in contact with the body fluids is utterly important for designing better biomaterials.

2. Materials and methods

Three TiZr alloy samples with 50 wt.% Zr and 50 wt.% Ti, purchased from ATI Wah Chang Co. were polished with corundum (Al_2O_3) abrasive paper grit 100, 120, 180, 240, 320, 400 and 800. After polishing, the samples were washed with hexane, ethanol and ultrapure water.

The corrosion behavior of the Ti50Zr samples was evaluated in simulated body fluid (SBF) with various concentrations of bovine serum albumin (BSA). The SBF was chosen because it contains phosphate ions, one of the most important minerals of biological hard tissues. The BSA concentrations were chosen based on the concentrations found in the human interstitial fluid [25]. Electrochemical testing was performed after immersing the samples in solutions for one hour. For the ICP-MS and UV/Vis analysis, the samples were placed in closed containers containing SBF with no albumin, with 0.5 g/L albumin and 1.0

g/L albumin, respectively and were kept up to 98 days. The pH of the solution was 7.40 at 36.5 °C. The protocol followed for SBF solution preparation was described by Kokubo and Takadama [26], obtaining the composition presented in Table 1. All the materials used were of analytical purity, BSA was provided as lyophilized powder (≥98%) from SigmaAldrich Inc.

Table 1

Chemical composition of SBF solution

Ion	Na^+	K^+	Mg^{2+}	Ca^{2+}	Cl^-	HCO_3^-	HPO_4^{2-}	SO_4^{2-}
Concentration (mM)	142.0	5.0	1.5	2.5	147.8	4.2	1.0	0.5

For the determination of the metal ions concentrations was used an Agilent 7800 Quadrupole ICP-MS instrument, equipped with an Octopole Reaction System (ORS) cell that was used in helium (He) collision mode to eliminate the polyatomic interferences. The method parameters are described in Table 2.

Table 2

ICP-MS method parameters

RF Power	1550 W
RF Matching	1.30 V
S/C Temp	2°C
Plasma Gas	15.0 L/min
Nebulizer Gas	1.07 L/min
Auxiliary Gas	0.90 L/min
He Flow	4.3 L/min

For the spectroscopic analysis, it was used a UV/Vis spectrophotometer SPECORD 200 PLUS from Analytik Jena. Electrochemical measurements were performed with Autolab (PGSTAT N301).

The electrochemical corrosion tests were carried out using a conventional three-electrode electrochemical cell. The Ti50Zr samples were used as working electrode, while a Pt electrode was used as a counter electrode. As reference electrode was used the Ag/AgCl ($[Cl^-]$=4M) electrode. Each electrochemical corrosion test was repeated at least three times.

The potentiodynamic polarization (PDP) and electrochemical impedance spectroscopy (EIS) measurements have been conducted to evaluate the behavior of Ti50Zr in the presence of BSA and also to study the adsorption of BSA on the surface.

PDP tests were conducted in a potential range of -0.25 V vs. OCP to 1 V vs. Ag/AgCl with a scan rate of 0.167 mVs^{-1}. The corrosion mechanism of the passive film at the film/electrolyte interface was investigated by EIS. The measurements were performed with the amplitude of 10 mV at OCP in the frequency range of 0.01 to 10,000 Hz and a sampling rate of 10 points per decade. Data were fitted using the software NOVA 1.6.

3. Results and discussions

The polarization behavior of the Ti50Zr alloy samples in the SBF solutions without and with albumin is presented in Fig. 1. The cathodic polarization behaviors of the three Ti50Zr samples were similar, meaning that the cathodic behavior is due to oxygen evolution.

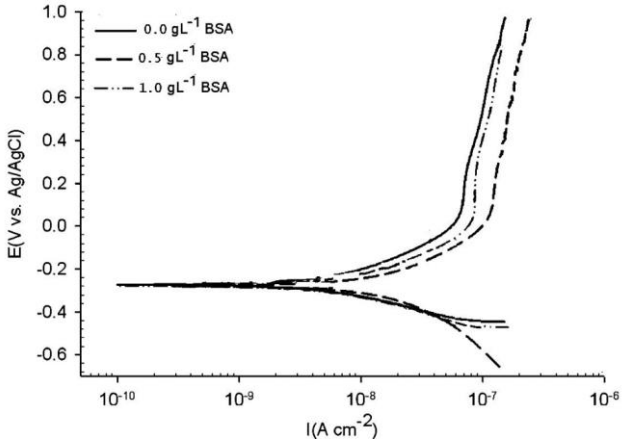

Fig. 1. Polarization plots for the three Ti50Zr alloy samples in SBF at different albumin concentrations

The PD studies have shown that a breakdown potential was not detected for the Ti50Zr samples up to 1 V vs. Ag/AgCl. The electrochemical parameters: the corrosion potential (E_{cor}), and the corrosion current (I_{cor}) are presented in table 1.

Table 3

Electrochemical parameters for Ti50Zr samples in SBF solution with BSA additions

BSA (gL^{-1})	E_{cor} (mV vs Ag/AgCl)	I_{cor} (μAcm^{-2})	v_{cor}($\mu myear^{-1}$)
0	-234 ±0.03	0.25±0.03	1.8 ± 0.3
0.5	-249 ±0.05	0.18±0.06	0.9 + 0.2
1	-260 ±0.02	0.12±0.05	1.4 ± 0.3

The stability of the titanium alloys passive layer can be evaluated through the interaction between the outer passive layer and the solution [27]. In the case of

Ti50Zr, the oxide layer contains TiO, Ti_2O_3 and TiO_2, respectively, the outer layer being enriched with ZrO_2 [6, 28–30]. Chemisorption of water on the surface of TiO_2 produces two types of surface hydroxyl groups [31]. Phosphate ions ($H_2PO_4^-$, HPO_4^{2-}) can bind to titanium ions in exchange reactions with the hydroxyl groups. The chemical adsorption of BSA onto the TiO_2 depends on the number of hydroxyl groups from the surface and on the total surface energy given by the values of the polar components [32, 33]. From the electrochemical parameters we can see a decrease in the corrosion current with the increase of albumin concentration in SBF, after immersion in solution for one hour. This can be explained either by an increase in the stability of the passive film on the surface of the Ti50Zr alloy or by the creation of an adsorption layer due to the presence of BSA in solution.

The rate of protein adsorption depends on the growth of the oxide layer, on the surface of titanium [34] and on the crystalline form of the TiO_2 [35]. To investigate if the BSA formed a film on the surface in time, the concentration of albumin was analyzed spectrophotometrically in the solutions prepared. Firstly, the calibration solutions were spectrally analyzed (190 – 800 nm) to confirm the maximum absorbance peak (280 nm). The spectra are presented in Fig. 2. Secondly, a calibration curve was constructed in the range 0.01 g/L – 0.08 g/L at 280 nm, which is presented in Fig. 3.

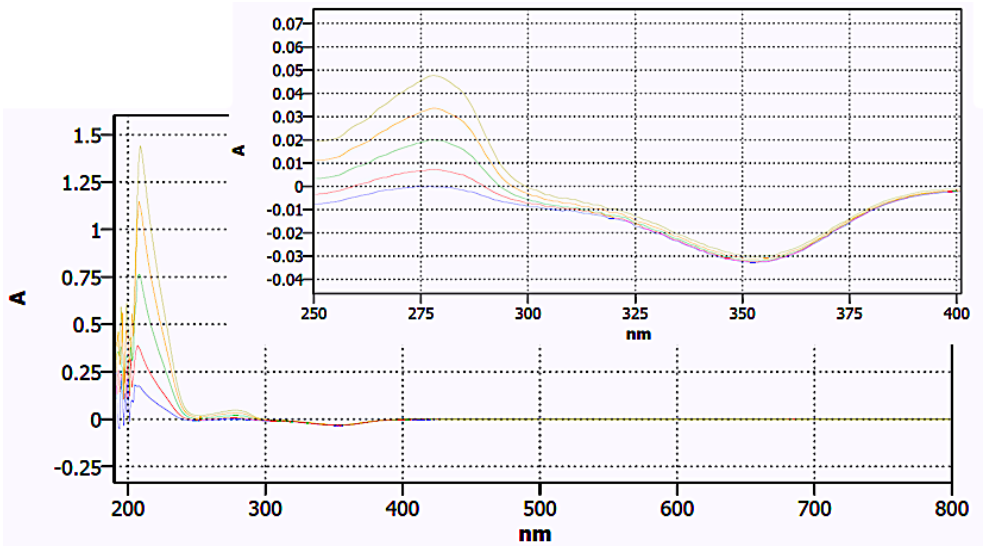

Fig. 2. Spectra of albumin solutions (0.01 g/L – 0.08 g/L)

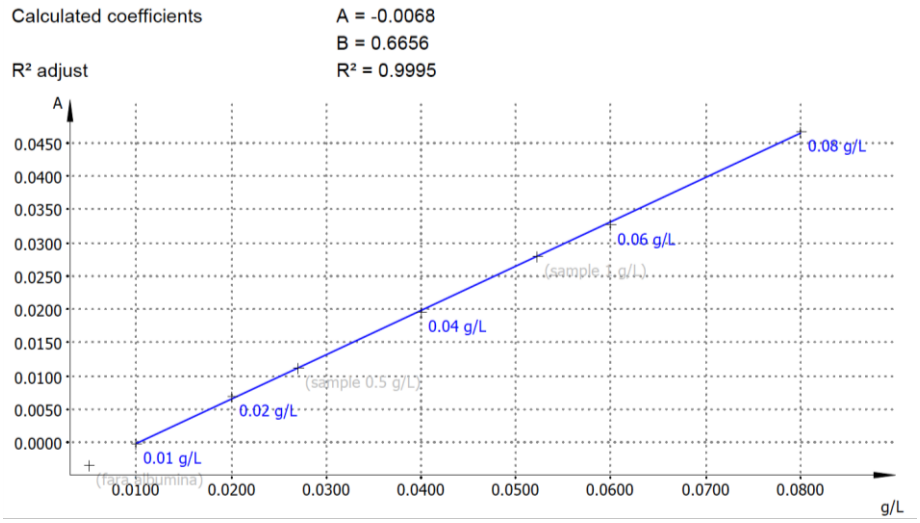

Fig. 3. Albumin calibration curve (0.01 g/L – 0.08 g/L)

The calibration curves of Ti and Zr for the ICP-MS determination were constructed in the range 0.1 ppb – 5.0 ppb and their graphical representation is presented in Fig. 4.

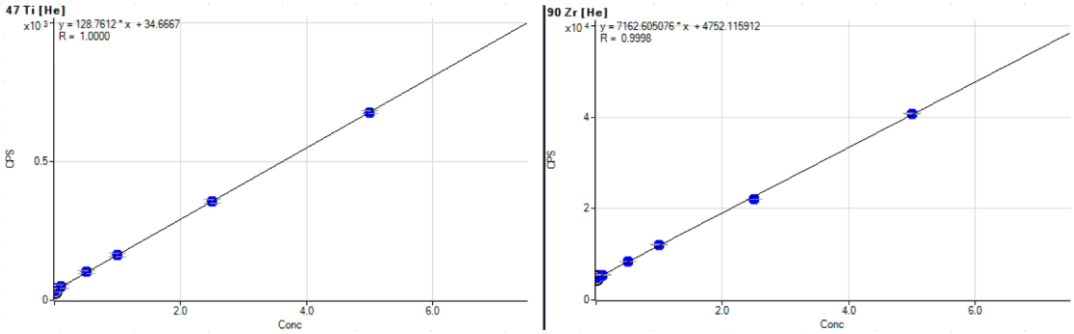

Fig. 4. Calibration curve for Ti and Zr (0.1 ppb - 5.0 ppb)

The SBF solutions with their corresponding concentration of albumin in which the Ti50Zr samples were placed, were analyzed starting after the first 4h of immersion each day for an initial period of 28 days, after which the samples were analyzed at longer intervals up to 98 days. The concentration of both Ti and Zr were in the range of parts per billion (ppb).

The spectrophotometric analysis was performed only in the last stage to see if adsorption took place on the metal surface. The results obtained are presented in Table 4.

After the first 4h from immersion, Ti concentration was around 4 ppb in all three solutions, decreasing slightly along with the increase in albumin

concentration. Zr concentration, compared with Ti, was 10 times lower in the solution with no albumin and 20 times lower in the solution with 0.5 g/L albumin, while in the solution with 1.0 g/L albumin, Zr was not detected. This trend has been observed throughout the entire period. The albumin concentration in solutions was determined starting with day 77. In both solutions that contained albumin was detected a smaller concentration than the initial one, which was observed to continuously decrease in time, indicating adsorption on the alloy surface. From the combined ICP-MS and UV/Vis analysis it is suggested that albumin has been adsorbed on the Ti50Zr surface and that it acts as a barrier by inhibiting the corrosion process.

Table 4

Results obtained

Day	Ti50Zr without albumin			Ti50Zr – 0.5 g/L albumin			Ti50Zr – 1.0 g/L albumin		
	Ti (ppb)	Zr (ppb)	Albumin (g/L)	Ti (ppb)	Zr (ppb)	Albumin (g/L)	Ti (ppb)	Zr (ppb)	Albumin (g/L)
1 (4h)	4.5 ± 0.54	0.4 ± 0.03	-	4.2 ± 0.50	0.2 ± 0.02	-	3.5 ± 0.42	-	-
7	4.5 ± 0.54	0.5 ± 0.04	-	4.8 ± 0.58	0.2 ±0.02	-	3.8 ± 0.46	-	-
14	4.5 ± 0.54	0.5 ± 0.04	-	4.8 ± 0.58	0.2 ±0.02	-	4.0 ± 0.48	-	-
28	5.9 ± 0.71	0.5 ± 0.04	-	5.4 ± 0.65	0.2 ±0.02	-	4.3 ± 0.52	-	-
56	8.2 ± 0.98	0.5 ± 0.04	-	5.9 ± 0.71	0.2 ±0.02	-	4.5 ± 0.54	-	-
77	13.1 ± 1.57	0.5 ± 0.04	-	12.3 ± 1.48	0.2 ±0.02	0.45 ± 0.02	7.4 ±0.89	-	0.87 ± 0.03
84	13.2 ± 1.58	0.5 ± 0.04	-	12.5 ± 1.50	0.2 ±0.02	0.31 ± 0.01	7.8 ± 0.94	0.1 ± 0.01	0.83 ± 0.03
91	14.5 ± 1.74	0.7 ± 0.06	-	13.5 ± 1.62	0.2 ±0.02	0.29 ± 0.01	7.8 ± 0.94	0.1 ± 0.01	0.79 ± 0.03
98	14.6 ± 1.75	0.8 ± 0.06	-	14.2 ± 1.70	0.2 ±0.02	0.23 ± 0.01	7.9 ± 0.95	0.2 ± 0.02	0.75 ± 0.03

The Bode diagrams for the Ti50Zr alloy samples in SBF solutions containing different amounts of BSA concentrations at 37 °C are presented in Fig. 5. The absolute impedance data was independent of frequency from 10^4 down to 10^3 Hz. This frequency range showed a resistive behavior corresponding to the solution resistance between the working and the reference electrode.

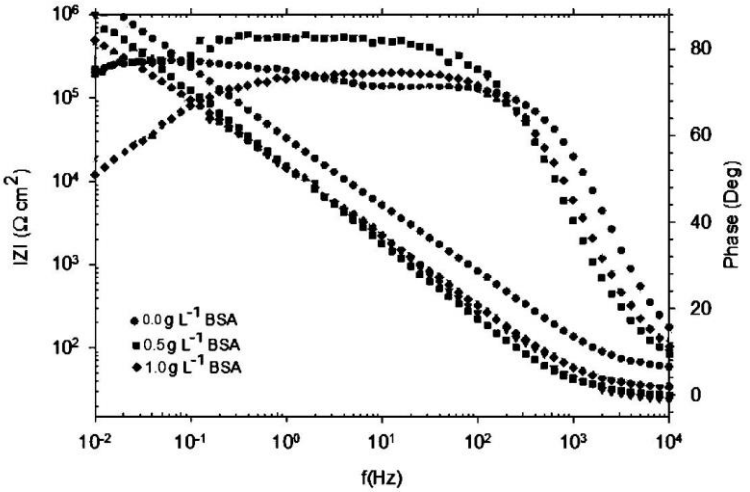

Fig. 5. Bode diagrams of the three Ti50Zr alloy samples after 1 hour of immersion at open circuit potential with various BSA amount

In the frequency range of 100 to 0.1Hz the phase angle value reached the maximum value around 80^0. In this frequency range, the phase angle values were independent of frequency while the absolute impedance values were increasing indicating a passive behavior of Ti50Zr samples. In the frequency range of 0.1 to 0.01Hz the absolute impedance increased, and the phase angle shifted to lower values. The presence of BSA in the SBF solution leads to decrease in absolute impedance magnitude. In Fig. 6 is shown a typical Nyquist diagram for the Ti50Zr alloy samples in SBF solutions containing different BSA concentrations at 37°C.

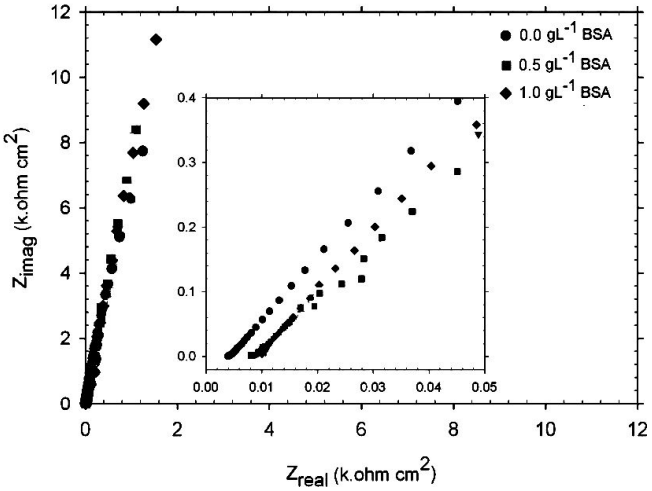

Fig. 6. Nyquist diagrams of the three Ti50Zr alloy samples after 1 hour of immersion at OCP in with BSA

The Nyquist curves showed a one-time constant. The proposed equivalent circuit used for fitting the experimental results presented in Fig. 7, is widely used for Ti alloys [36]. In this circuit, R_s is the solution resistance between the working and the reference electrode and R_b and CPE are the resistance and capacitance of the barrier layer. For the mathematical analysis of impedance diagrams, a constant phase element (CPE) is used instead of a pure capacitor to consider the non-uniform current distribution due to surface roughness and non-homogeneities related to BSA adsorption [37].

The impedance of CPE is described by the following formula:

$$Z_{CPE}=\frac{1}{(j\omega)^{n_c}Y_0} \quad (1)$$

The exponent n_c is a coefficient related to the deviation between real capacitance and pure capacitance, Y_0 is the general admittance function, and ω represents the angular frequency. The magnitude of the electrical circuit parameters was simulated by ZSimpWin software. All impedance parameters are shown in Table 5. The fitting quality was evaluated by chi-squared ($\chi 2$). The values obtained were less than 4×10^{-3}, indicating a satisfactory fit.

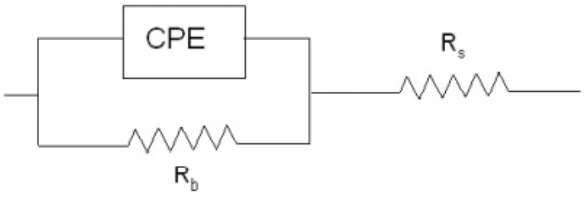

Fig. 7. Proposed electrical circuits for the Ti50Zr alloy samples after one hour immersion in SBF solutions with various BSA concentrations

Table 5

Electrochemical parameters of the equivalent circuits obtained for the three Ti50Zr alloy samples after one hour immersion in SBF solutions with various BSA concentrations

samples	$R_s[\Omega cm^2]$	$Rp[k\Omega cm^2]$	$Y_0[\mu\Omega^{-1}S^n cm^{-2}]$	n_c	$\chi^2\times10^{-4}$
Ti50Zr/SBF+0.0gL^{-1}BSA	8.6	160.6	90.8	0.96	4.28
Ti50Zr/SBF+0.5gL^{-1}BSA	12.2	280.5	32.9	0.92	8.25
Ti50Zr/SBF+1.0gL^{-1}BSA	14.1	272.4	39.4	0.88	3.88

The results obtained by the EIS show an increase in polarization resistance. This means an increased thickness of the barrier layer resulted from the addition of BSA.

4. Conclusions

From the combined experimental data, we have observed that the addition of BSA in SBF led to the formation of a thicker outside layer, which most likely formed through the adsorption of BSA on the naturally occurring oxide layer of the Ti50Zr alloys used. Moreover, an increase in the stability of the passive film was observed that also translated into lower concentrations of metal ions released in the solutions analyzed, indicating that the layer formed acts as a barrier inhibiting corrosion. Although the "in vivo" conditions are arduous to mimic, the results obtained indicate furthermore that the Ti50Zr alloy is a promising biomaterial.

REFERENCES

[1]. *A. Sharma, J.N. Waddell, K.C. Li, L. A Sharma, D.J. Prior, W.J. Duncan*, Is titanium–zirconium alloy a better alternative to pure titanium for oral implant? Composition, mechanical properties, and microstructure analysis, Saudi Dental Journal, 2020, pp. 4–11;

[2]. *D. Ionita, C. Pirvu, A.B. Stoian, I. Demetrescu*, The Trends of TiZr Alloy Research as a Viable Alternative for Ti and Ti16 Zr Roxolid Dental Implants, Coatings, **vol. 10**, no. 4, 2020, p. 422;

[3]. *M. Vardaki, A. Pantazi, I. Demetrescu, M. Enachescu*, Assessing the Functional Properties of TiZr Nanotubular Structures for Biomedical Applications, through Nano-Scratch Tests and Adhesion Force Maps, Molecules, **vol. 26**, no. 4, 2020, p. 900;

[4]. *M. Prodana, C.E. Nistor, A.B. Stoian, D. Ionita, C. Burnei*, Dual nanofibrous bioactive coatings on TiZr implants, Coatings, **vol. 10**, no. 6, 2020, pp. 1–16;

[5]. *S. Roehling, M. Astasov-Frauenhoffer, I. Hauser-Gerspach, et al.*, In Vitro Biofilm Formation on Titanium and Zirconia Implant Surfaces, Journal of Periodontology, **vol. 88**, no. 3, 2017, pp. 298–307;

[6]. *I. Demetrescu, C. Dumitriu, G. Totea, C.I. Nica, A. Dinischiotu, D. Ionita*, Zwitterionic cysteine drug coating influence in functionalization of implantable Ti50Zr alloy for antibacterial, biocompatibility and stability properties, Pharmaceutics, **vol. 10**, no. 4, 2018, p. 220;

[7]. *A. Sharma, A.J. McQuillan, Y. Shibata, L.A. Sharma, J.N. Waddell, W.J. Duncan*, Histomorphometric and histologic evaluation of titanium–zirconium (aTiZr) implants with anodized surfaces, Journal of Materials Science: Materials in Medicine, **vol. 27**, no. 5, 2016, p. 86;

[8]. *T. Hanawa*, Biofunctionalization of titanium for dental implant, Japanese Dental Science Review, **vol. 46**, no. 2, 2010, pp. 93–101;

[9]. *P. Silva-Bermudez, S.E. Rodil*, An overview of protein adsorption on metal oxide coatings for biomedical implants, Surface and Coatings Technology, **vol. 233**, 2013, pp. 147–158;

[10]. *D. Bajenaru-Georgescu, D. Ionita, M. Prodana, I. Demetrescu*, Electrochemical and antibacterial characterization of thermally treated titanium biomaterials, UPB Scientific Bulletin, Series B: Chemistry and Materials Science, **vol. 77**, no. 4, 2015, pp. 63–74;

[11]. *C. Valero Vidal, A. Igual Muñoz*, Influence of protein adsorption on corrosion of biomedical alloys, Woodhead Publishing Limited, 2013, pp. 187-219;

[12]. *M. Talha, Y. Ma, P. Kumar, Y. Lin, A. Singh*, Role of protein adsorption in the bio corrosion of metallic implants – A review., Colloids and Surfaces B: Biointerfaces, **vol.**

176, 2019, pp. 494–506;
[13]. *O. Klok, A.I. Munoz, S. Mischler*, An overview of serum albumin interactions with biomedical alloys, Materials, **vol. 13**, no. 21, 2020, pp. 1–26;
[14]. *S. Höhn, S. Virtanen, A.R. Boccaccini*, Protein adsorption on magnesium and its alloys: A review, Applied Surface Science, **vol. 464**, 2019, pp. 212–219;
[15]. *V. Wagener, A.S. Faltz, M.S. Killian, P. Schmuki, S. Virtanen*, Protein interactions with corroding metal surfaces: Comparison of Mg and Fe, Faraday Discussions, **vol. 180**, 2015, pp. 347–360;
[16]. *J. Barberi*, Titanium and Protein Adsorption : An Overview of Mechanisms and Effects of Surface Features, Materials, **vol. 14,** no. 7, 2021, p. 1590;
[17]. *Z. Wang, Y. Yan, L. Qiao*, Protein adsorption on implant metals with various deformed surfaces, Colloids and Surfaces B: Biointerfaces, **vol. 156**, 2017, pp. 62–70;
[18]. *Y. Hedberg, X. Wang, J. Hedberg, M. Lundin, E. Blomberg, I. Odnevall Wallinder*, Surface-protein interactions on different stainless steel grades: Effects of protein adsorption, surface changes and metal release, Journal of Materials Science: Materials in Medicine, **vol. 24**, no. 4, 2013, pp. 1015–1033;
[19]. *B. Alemón, M. Flores, W. Ramírez, J.C. Huegel, E. Broitman*, Tribocorrosion behavior and ions release of CoCrMo alloy coated with a TiAlVCN/CNx multilayer in simulated body fluid plus bovine serum albumin, Tribology International, **vol. 81**, no. 81, 2015, pp. 159–168;
[20]. *D. Ionita, F. Golgovici, I. Demetrescu, M. Sajin, G.R. Pandelea-Dobrovicescu*, Effect of human albumin on corrosion and biological behavior of CoCrMo, Materials and Corrosion, **vol. 68**, no. 8, 2017, pp. 876–882;
[21]. *H.H. Huang*, Effect of fluoride and albumin concentration on the corrosion behavior of Ti-6Al-4V alloy, Biomaterials, **vol. 24**, no. 2, 2003, pp. 275–282;
[22]. *S. Omanovic, S.G. Roscoe*, Electrochemical studies of the adsorption behavior of bovine serum albumin on stainless steel., Langmuir, **vol. 15**, no. 23, 1999, pp. 8315–8321;
[23]. *Y.S. Hedberg*, Role of proteins in the degradation of relatively inert alloys in the human body, npj Materials Degradation, **vol. 2**, no. 1, 2018, pp. 1–5;
[24]. *H. Matusiewicz*, Potential release of in vivo trace metals from metallic medical implants in the human body: From ions to nanoparticles - A systematic analytical review, Acta Biomaterialia, **vol. 10**, no. 6, 2014, pp. 2379–2403;
[25]. *A. Kuhn, P. Neufeld, T. Rae*, Synthetic Environments for the Testing of Metallic Biomaterials, In: The Use of Synthetic Environments for Corrosion Testing, ASTM International, 100 Barr Harbor Drive, PO Box C700, West Conshohocken, PA 19428-2959 (1986), pp. 79-79-19;
[26]. *T. Kokubo, H. Takadama*, How useful is SBF in predicting in vivo bone bioactivity?, Biomaterials, **vol. 27**, no. 15, 2006, pp. 2907–2915;
[27]. *M. Pourbaix*, Electrochemical corrosion of metallic biomaterials, Biomaterials, **vol. 5**, no. 3, 1984, pp. 122–134;
[28]. *X. Liu, P.K. Chu, C. Ding*, Surface nano-functionalization of biomaterials, Materials Science and Engineering R: Reports, **vol. 70**, no. 3–6, 2010, pp. 275–302;
[29]. *N.T.C. Oliveira, S.R. Biaggio, S. Piazza, C. Sunseri, F. Di Quarto*, Photo-electrochemical and impedance investigation of passive layers grown anodically on titanium alloys, Electrochimica Acta, **vol. 49**, no. 26, 2004, pp. 4563–45761;
[30]. *H. Habazaki, M. Uozumi, H. Konno, K. Shimizu, S. Nagata, K. Asami, K. Matsumoto, K. Takayama, Y. Oda, P. Skeldon, G.E. Thompson*, Influences of structure and composition on growth of anodic oxide films on Ti-Zr alloys, Electrochimica Acta, **vol. 48**, no. 20–22, 2003, pp. 3257–32661;
[31]. *H.P. Boehm*, Acidic and basic properties of hydroxylated metal oxide surfaces,

Discussions of the Faraday Society, **vol. 52**, 1971, p. 264;
[32]. *M.J. Desroches, N. Chaudhary, S. Omanovic*, PM-IRRAS Investigation of the Interaction of Serum Albumin and Fibrinogen with a Biomedical-Grade Stainless Steel 316LVM Surface, Biomacromolecules, **vol. 8**, no. 9, 2007, pp. 2836–2844;
[33]. *D. Ionita, R. Popescu, T. Tite, I. Demetrescu*, The Behaviour of Pure Titanium in Albumin Solution, Molecular Crystals and Liquid Crystals, **vol. 486**, no. 1, 2008, pp. 166/[1208]-174/[1216];
[34]. *M.C. Sunny, C.P. Sharma*, Titanium-Protein Interaction: Changes with Oxide Layer Thickness, Journal of Biomaterials Applications, **vol. 6**, no. 1, 1991, pp. 89–98;
[35]. *E. Jia, X. Zhao, Y. Lin, Z. Su*, Protein adsorption on titanium substrates and its effects on platelet adhesion, Applied Surface Science, **vol. 529**, 2020, p. 146986;
[36]. *A. Mazare, M. Dilea, D. Ionita, I. Titorencu, V. Trusca, E. Vasile*, Changing bioperformance of TiO2 amorphous nanotubes as an effect of inducing crystallinity, Bioelectrochemistry, **vol. 87**, 2012, pp. 124–131;
[37]. *C.L. Liu, Y.J. Wang, M. Wang, W.J. Huang, P.K. Chu*, Electrochemical behaviour of TiO 2 nanotube on titanium in artificial saliva containing bovine serum albumin, Corrosion Engineering, Science and Technology, **vol. 47**, no. 3, 2012, pp. 167–169;